ISSN 1022 - 2502, E-ISSN 2408- 8528
Dhaka Univ. J. Sci. 72(1): 85-91, 2024 (January) DOI: https://doi.org/10.3329/dujs.v72i1.71196

Numerical Analysis of Various Types of Flows Over NACA 4415 Airfoil

Md. Lutfar Rahman Sarkar[1,2] and M. Z. I. Bangalee[1,2*]

[1] *Department of Applied Mathematics, University of Dhaka, Dhaka-1000, Bangladesh*
[2] *Research group of Fluid Flow Modeling and Simulation*
Department of Applied Mathematics, University of Dhaka, Dhaka-1000, Bangladesh

(Received : 11 October 2023 ; Accepted: 13 December 2023)

Abstract

Because of the high-speed aircrafts, the distance to the other side of the world seems to be closer, as if it were situated just next door. Aerospace engineering has undergone a revolution thanks to research into airfoils. This research work has been focused on analyzing the aerodynamic performances of the NACA 4415 airfoil in turbulent flows while Mach numbers, 0.2,0.6 and Reynolds numbers, $3 \times 10^6, 2.17 \times 10^5$ have been taken into account. The chord length of 647mm and 152mm have been considered for this study. Computational fluid dynamics were employed to determine the lift, drag, and pitching moment forces, as well as their respective non-dimensional coefficients. As a result, maximum lift, moment forces have been found after the 16° angle of attacks, and stagnation areas are increasing dramatically behind the airfoil, proportion to the increments with the angle of attack. Additionally, the effects of pressure and velocity on every point of the airfoil's surface were studied through the analysis of pressure and velocity contours.

Keywords: Aerodynamics, Airfoil, CFD, Lift, Drag, Moment, Pressure, Velocity;

I. Introduction

At the turn of the 20th century, powered flight became a reality, and the significance of aerodynamics increased dramatically. As a result, research into the aerodynamic behavior of lifting surfaces like fixed wings on aeroplanes and later, rotors on helicopters, became more and more popular. When Ludwig Prandtl and his colleagues at Gottingen, Germany, demonstrated that the aerodynamic consideration of wings could be divided into two parts: (1) the study of a wing's section, an airfoil, and (2) the fixation of such airfoil properties to account for the complete, finite wing, the analysis of aeroplane wings advanced significantly between 1912 and 1918. This method is still in use today; in fact, the National Aeronautics and Space Administration's (NASA) aeronautics research in the 1970s and 1980s included a significant amount of theoretical calculation and experimental measurement of the features of contemporary airfoils.

Airfoil is a two dimensional cross-sectioned area of three-dimensional wing. In 1884, Horatio F. Phillips patented the shapes of airfoil for the first time. Phillips, the Englishman named carried out the first significant wind tunnel tests on airfoils. The Wright brothers tested airfoils on their own in a wind tunnel in 1902, creating somewhat effective forms that helped them achieve their successful first flight on December 17, 1903. It is obvious that airfoil design in the early years of powered flight was essentially individualized and tailored. But around the beginning of the 1930s, NACA-the precursor to NASA-started a series of conclusive airfoil experiments using airfoil forms that were create logically and methodically. Today, several of these NACA airfoils are still in service.

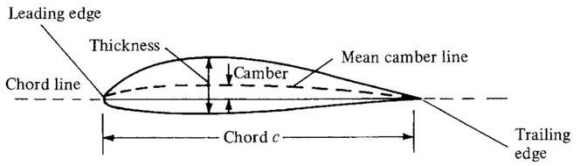

Fig. 1. Airfoil Nomenclature

Understanding the flow characteristics across the aircraft's lifting surfaces is one path to enhance the aerodynamic performances of the craft during cruising and manoeuvres. When the gradient of pressure is unfavourable, the boundary layer flow is typically stable at small Reynolds numbers, and this leads through laminar separation with or without turbulent reattachment. Without externally produced noises, the separation might extend beyond the airfoil's trailing edge, where it would significantly increase pressure drag[1]. The flow-control separation is therefore crucial, especially in cases of separation delay. To give the near-wall region more momentum, separation postponement uses the kernel[2]. One method for regulating flow separation on a number of aeroplanes in recent years has been the vortex generator (VG).

Numerous experimental and numerical studies of the VGs have been done. Several VG configurations have undergone testing to determine how well they manage flow. According to Godard et al.[3] and Betterton et al.[4], VG with distanced counter-rotating arrays seems more effective at postponing separation than co-rotating array forward wedges and linked counter-rotating devices. Wheeler[5] demonstrated that apexes pointing downstream are more effective at lowering drag and raising the airfoil stall angle than apexes pointing

*Author for correspondence. e-mail: zabid@du.ac.bd

forward, which disrupt the flow along the side wall. Numerous researchers have also studied the VGs parametrically. Godard[3], Pauley[6], and Ahmad[7], among others, discovered that the skewed angle of the VG will affect the skin friction and vortex strength downstream of the VG. Ahmad[8] and Bur et al.[9] have evaluated the impact of spacing between each pair of VGs in the interim. Several additional studies have investigated sub-VG, micro-VG, and blowing VG to examine their impact on flow management[10-13].

The flow behaviour above the airfoil with and without VGs has been better understood using computational fluid dynamics (CFD). The best flow devices are simple to develop using CFD. The findings of the CFD simulation demonstrated that passive VG is successful in reattaching the detached shear layer and minimizing the separation zone size[14]. Researchers have employed computational techniques to study turbulent boundary layer flow and vortex shedding using the large eddy simulation (LES) model and the Reynolds-averaged Navier-Stokes (RANS) model[15-16]. Johansen et al.[16] found that comparing the RANS model to typical LES models, it allowed for much coarser grids in the boundary layer and had a value that was pretty acceptable. Zhen et al.[17] used RANS and Spalart-Allmaras turbulence model for numerical methods and found satisfactory results compared to experimental data. They investigated that maximum lift coefficient increases when VGs are placed nearer to the separation point. Rectangular and curve edge VGs produce better result than triangular VGs.

The shape of the airfoil plays a major role in aerodynamic performance. Many different airfoil configurations have been employed for a variety of uses. In terms of aerodynamic performance, the airfoil still has some restrictions. By placing a slat next to the airfoil, you can enhance its aerodynamic performance. Slat is one of the passive flow controllers that is most frequently employed, particularly in aviation. Slats can add more lift force to an airfoil, increasing its lift capacity. As a passive flow control device, the slat can also be employed. By guiding the flow of fluid towards the main airfoil, the slat may regulate the flow. Slats can speed up the fluid flow in addition to guiding it. One result of the slat is that fluid flow re-circulation on the upper side of the airfoil can be diminished or even eliminated[18]. That re-circulation of flow is caused by the fluid flow separation[19]. The existence of fluid flow separation is harmful because it may result in an airfoil stall[20].

Airfoils and wings are topics of investigation. Both experimental and computational methods are used in it. Tank towing has been the subject of experimental investigation. Yavuz et al.[21] studied and claimed that using slats can increase maximum lift coefficient from $Cl_{\max} = 1.45$ to $Cl_{\max} = 2.78$. The stall conditions also increased from angle of attack $\alpha_{\text{stall}} = 16^{\circ}$ to $\alpha_{\text{stall}} = 24^{\circ}$. From this idea, Julian et al.[22] experimented on NACA 4415 airfoil by using single and double slat to investigate the aerodynamic performances. He found that stall condition occurred at the same angle of attack for both single and double slat. Though $Cl_{\max}$ increased by 25.69% for double slat where 20.91% for single slat. Change of Cd does not affect significantly for single slat. It produces double increment for double slat compare to single slat. In comparison to a double slat, a single slat can enhance an airfoil's aerodynamic performance. Without a slat, fluid flow separation forms on the upper side of the airfoil based on fluid flow visualization. Both single and double slats are effective at handling the fluid flow separation, although their effects are not radically different. In conclusion, single slats are preferable to double slats since they are more effective overall.

Based on an extensive and thorough review of the existing literature, it has been determined that our research endeavors will primarily focus on the meticulous examination of the aerodynamic characteristics associated with the regular NACA 4415 airfoil. This analysis will encompass two distinct chord lengths, as well as an innovative modified version of the NACA 4415 airfoil. The primary objective is to uncover and comprehensively understand the intricate nuances inherent to these airfoil configurations.

The investigation will center around the meticulous study of the lift, drag, and moment forces acting upon these airfoil designs, in conjunction with the corresponding dimensionless coefficients. It is firmly believed that these fundamental parameters are essential for obtaining a comprehensive and holistic understanding of the aerodynamic behavior exhibited by these airfoils.

To gain unparalleled insights into the underlying phenomena and establish a solid foundation for the analysis, the pressure, velocity, and modified turbulent viscosity contours associated with these airfoils will be meticulously scrutinized and analyzed. By doing so, a deeper appreciation and understanding of the intricate intricacies and complexities of the airflow patterns at varying angles of attack can be achieved. Consequently, a comprehensive elucidation of the aerodynamic behavior displayed by these airfoil configurations can be fostered.

The ultimate objective is to make some contributions to the existing knowledge in the field by enriching the understanding of aerodynamic performances and behavior

of the regular NACA 4415 airfoil. Through meticulous analysis and detailed visualization of the flow patterns, valuable insights will be provided for further research and development in the aerospace engineering domain.

II. Mathematical Modeling

Reynolds Averaging

For turbulence model, in the process of Reynolds averaging, the variables have been decomposed into two parts. One is mean variable, which is averaged by time and the other is fluctuation part. For velocity:

$$u_i = \bar{u}_i + u_i' \tag{1}$$

where $\bar{u}_i$ is mean velocity and u_i' is its fluctuating component.

By implementing the idea, we can also decompose any scalar quantity:

$$\phi = \bar{\phi} + \phi' \tag{2}$$

where ϕ can be any scalar quantity like pressure, temperature, energy or any relevant quantities.

By substituting such variables into continuity, momentum equations, and taking the averages with respect to time on these equations, dropping bar sign, we get:

$$\frac{\partial \rho}{\partial t} + \frac{\partial}{\partial x_i}(\rho u_i) = 0 \tag{3}$$

$$\begin{aligned} \frac{\partial}{\partial t}(\rho u_i) + \frac{\partial}{\partial x_j}\left(\rho u_i u_j\right) &= -\frac{\partial p}{\partial x_i} \\ + \frac{\partial}{\partial x_j}\left[\mu\left(\frac{\partial u_i}{\partial x_j} + \frac{\partial u_j}{\partial x_i} - \frac{2}{3}\delta_{ij}\frac{\partial u_l}{\partial x_l}\right)\right] \\ + \frac{\partial}{\partial x_j}\left(-\rho\overline{u_i' u_j'}\right) \end{aligned} \tag{4}$$

The above equations (3) - (4) are called Reynolds Averaged Navier-Stokes (RANS) equations. The term $-\rho\overline{u_i' u_j'}$ is called Reynolds stresses. A common approach to find values of the term is Boussinesq hypothesis[23].

$$\begin{aligned} -\rho\overline{u_i' u_j'} &= \mu_t\left(\frac{\partial u_i}{\partial x_j} + \frac{\partial u_j}{\partial x_i}\right) \\ &- \frac{2}{3}\left(\rho k + \mu_t \frac{\partial u_k}{\partial x_k}\right)\delta_{ij} \end{aligned} \tag{5}$$

It is used in Spalart-Allmaras, $k-\epsilon$ model, $k-\omega$ model. We are going to discuss about Spalart-Allmaras and $k-\epsilon$ turbulence models in following sections.

Spalart-Allmaras Turbulence Model

Spalart-Allmaras is a single modeled transport equation that calculates turbulence for viscosity and use it to measure modified turbulent viscosity. Aerodynamic flows were the subject of the Spalart-Allmaras model development. It does cause substantially bigger inaccuracies for some free shear flows, particularly plane and round jet flows, however it is not calibrated for ordinary industrial flows. Furthermore, it is unreliable for predicting how homogenous, isotropic turbulence may degrade.

The transport equation is:

$$\begin{aligned} \frac{\partial}{\partial t}(\rho\tilde{v}) + \frac{\partial}{\partial x_i}(\rho\tilde{v}u_i) &= G_v + \\ \frac{1}{\sigma_{\tilde{v}}}\left[\frac{\partial}{\partial x_j}\left\{(\mu + \rho\tilde{v})\frac{\partial\tilde{v}}{\partial x_j}\right\} + C_{b2}\rho\left(\frac{\partial\tilde{v}}{\partial x_j}\right)^2\right] \\ -Y_v + S_{\tilde{v}} \end{aligned} \tag{6}$$

Wall Boundary Conditions

With the addition of a y^+-insensitive wall treatment in ANSYS Fluent, a simulation software, the Spalart-Allmaras model has been expanded to include all of the solution variables from their viscous sublayer formulation

$$\frac{u}{u_\tau} = \frac{\rho u_\tau y}{\mu} \tag{7}$$

to the logarithmic layer of y^+

$$\frac{u}{u_\tau} = \frac{1}{\kappa}\ln E\left(\frac{\rho u_\tau y}{\mu}\right) \tag{8}$$

the notations are defined by as:

$u=$ Velocity parallel to the wall
$u_\tau=$ Friction velocity
$t=$ Distance from wall
$\kappa=$ von Karman constant
$E=$ Constant

Values of the constants are $\kappa = 0.4187$ and $E = 9.793$.

$k-\epsilon$ Turbulence Model

Up until the last decade of the twentieth century, the $k-\epsilon$ model was the most often used two-equation model. Chou[24], Davidov[25], and Harlow and Nakayama[26] made the first development attempts based on this paradigm. The version of the model introduced by Jones and Launder[27] marked the beginning of its widespread use. Later, Launder and Sharma[28] "retuned" the closure

coefficients of the model and developed what is known as the Standard $k-\epsilon$ model[29].

By solving two different transport equations, two-equations turbulence models enable the estimation of both, the turbulent length and the scale of time. Since, fluent has emerged as the workhorse of real-world flow calculations. Its prevalence in industrial flow and heat transfer simulations can be attributed to its robustness, economy, and tolerable accuracy for a variety of turbulent flows. It is semi-empirical model, and the model equations are derived using phenomenological considerations and empirical evidence.

The $k-\epsilon$ model is a transportation equation consisting of two equations for turbulence phenomena where k is derived from the exact equation and ϵ is derived considering physical phenomena occured. In addition, the model was derived for fully turbulent flow where molecular viscosity has negligible effects. So, mainly k represents the kinetic energy where ϵ has the meaning of viscous dissipation rate.

The equations that can be determined for kinetic energy, k and the rate of dissipation, ϵ are:

$$\frac{\partial}{\partial t}(\rho k)+\frac{\partial}{\partial x_i}(\rho k u_i)=\frac{\partial}{\partial x_j}\left[\left(\mu+\frac{\mu_t}{\sigma_k}\right)\frac{\partial k}{\partial x_j}\right] +G_k+G_b-\rho\epsilon-Y_m+S_k \tag{9}$$

and

$$\frac{\partial}{\partial t}(\rho \epsilon)+\frac{\partial}{\partial x_i}(\rho \epsilon u_i)=\frac{\partial}{\partial x_j}\left[\left(\mu+\frac{\mu_t}{\sigma_\epsilon}\right)\frac{\partial \epsilon}{\partial x_j}\right] +C_{1\epsilon}\frac{\epsilon}{k}(G_k+C_{3\epsilon}G_b)-C_{2\epsilon}\rho\frac{\epsilon^2}{k}+S_\epsilon \tag{10}$$

III. Results and Discussion

To ensure the validity of this research work, the numerical results have been compared with some research papers. At first, lift coefficients have been validated with Zhen et al.[17], Pope & Harper[30], Efstratios[31], Fouatih et al.[32]

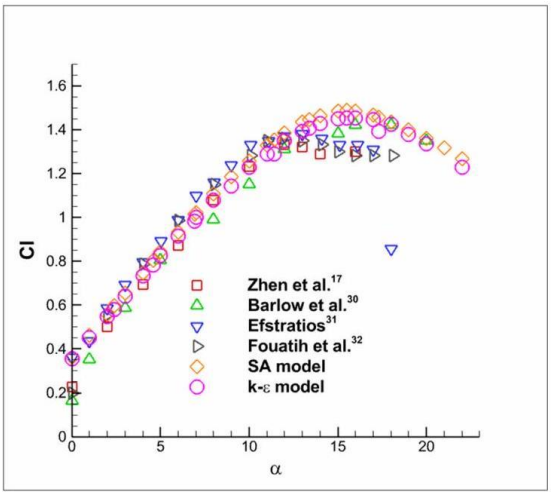

Fig. 2. Comparison of C_L at Various α

Now, drag coefficients have been compared with Pope & Harper[30].

The numerical comparisons of two aerodynamic non-dimensional coefficients

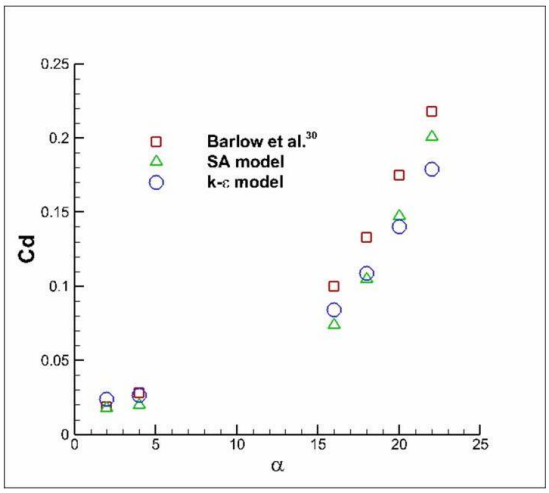

Fig. 3. Comparison of C_d at Various α

are the proof of the validity of this research work. Now, some other numerical findings are given below.

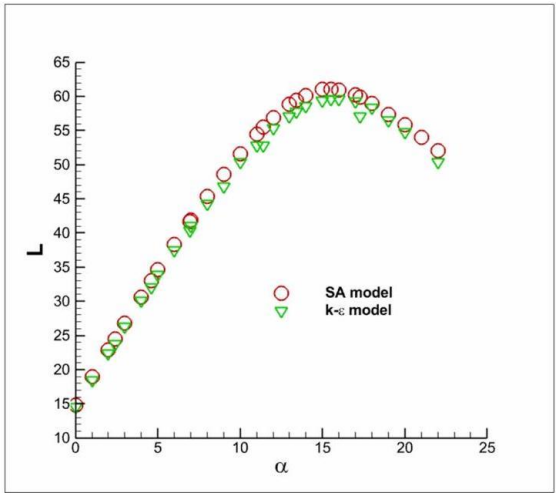

Fig. 4. Lift force at different α

The figures show the numerical data of lift and moment forces according to Sapalart-Allmaras and $k-\epsilon$ turbulence model. It is clearly shown that lift and moment forces increase uniformly till 15° and starts decreasing after that angle of attack. It proves that the stall condition is situated at such angle. At post stall condition, it is obvious that these forces lose

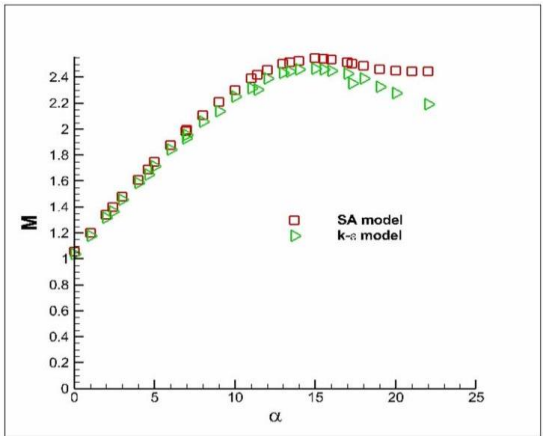

Fig. 5. Pitching moment force at different α

their values due to bluff condition.

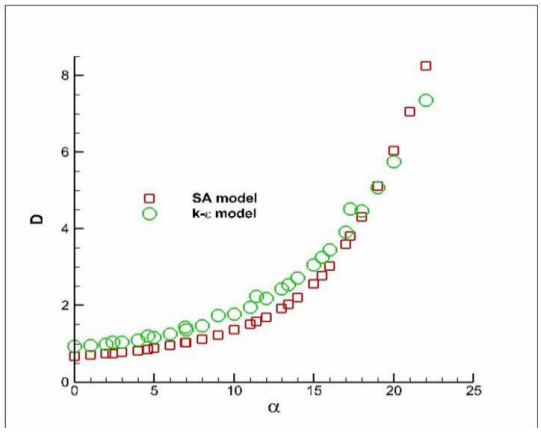

Fig. 6. Drag force at different α

The drag forces increase gradually with the increments of the angle of attack. The surfaces of the airfoil experience more resistance of air flow for high angle of attack, especially at post stall condition. The chaotic behavior of the unstable body causes such phenomena.

By getting the model validation for 152mm of chord length, the extended work is to find some contours for another chord length, 647mm

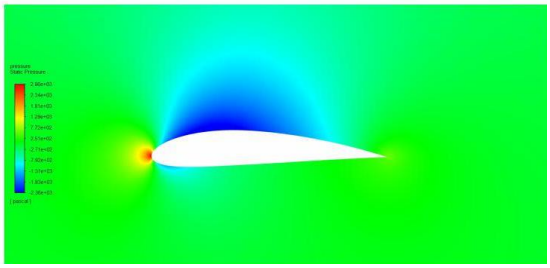

Fig. 7. Pressure contour at $\alpha = 0^{\circ}$

The maximum pressure has been found where the flow interacts directly to the airfoil surface. This is the reason to get maximum pressure at the leading edge of the airfoil. The upper surface experience the minimum pressure at such occurrence.

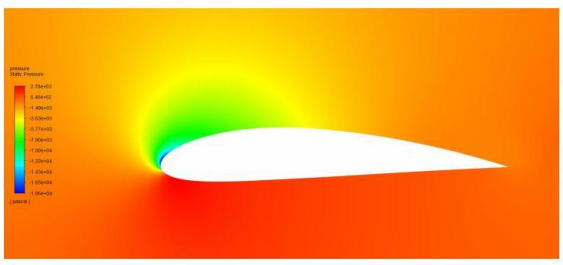

Fig. 8. Pressure contour at $\alpha = 16^{\circ}$

At high angle of attack, the air flow interacts at lower surface of the airfoil. This causes to find high pressures at the bottom of the airfoil. The low pressure is found at just the upper surface of leading edge.

By focusing at the velocity at every point of the airfoil surface, contrasts have been found to velocity contours, comparing to pressure contours.

The minimum velocity has been found where fluid flow comes to attack directly to the airfoil surface. Zero velocity is found there and it is called total condition. For low angle of attack, e.g. $\alpha = 1°$, total condition is found almost at the leading edge of the airfoil. The maximum velocity has been

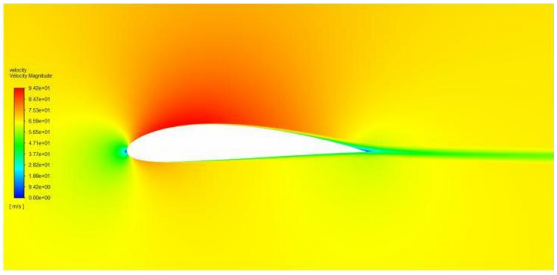

Fig. 9. Velocity contour at $\alpha = 1°$

found at the upper surface of the airfoil.

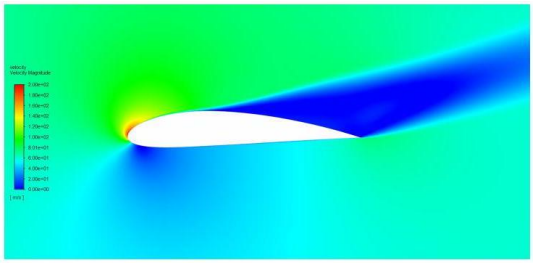

Fig. 10. Velocity contour at $\alpha = 22°$

At very high angle of attack, for $\alpha = 22°$, the total condition is found at the lower surface of the surface. The maximum pressure has been found just upper side of the leading edge. At such high angle of attack, a huge stagnation area has been discovered behind the trailing edge. At post stall condition, since the airfoil becomes a bluff body and it starts to fall, it left a vacuum region just behind its trailing edge.

IV. Conclusions

To sum up by analyzing the aerodynamic performances of the NACA 4415 airfoil, the stall condition has been found in the angle between 16° and 17°. In addition, lift and moment forces, according to their dimensionless coefficients, increase till that angle and starts declining after incrementing the angle. Furthermore, the graph of drag forces rise up dramatically at post stall angles. However, the maximum pressure has been found where the fluid flow interacts directly to the airfoil surfaces. On the other hand, velocity show the opposite characteristics. Finally, the velocity contours provide the information about the huge stagnation area at high angles of attack which have been found behind the trailing edge. This knowledge could be implemented while manufacturing aircraft with the NACA 4415 airfoil.

Acknowledgement

We are highly grateful to Centennial Research Grant, University of Dhaka and the University Grants Commission of Bangladesh for providing the financial support. This work was also supported by the Bose center for Advanced Study and Research in Natural Sciences, University of Dhaka, and the fellowship granted by the ministry of science and technology, Bangladesh.

References

1. Stack, J.P. and S. M. Mangalam, 1990. Method and apparatus for detecting laminar flow separation and reattachment. National Aeronautics and Space Administration NASA, U.S. Patent **4**, 936, 146.
2. Shan, H., L. Jiang, C. Liu, M. Love, and B. Maines, 2008. Numerical study of passive and active flow separation control over a NACA0012 airfoil. Journal of Computers E fluids, **37(8)**, 975-992.
3. Godard, G. and M. Stanislas, 2006. Control of a decelerating boundary layer. Part 1: Optimization of passive vortex generators. Journal of Aerospace Science and Technology, **10(3)**, 181-191.
4. Betterton, J.G., K. C. Hackett, P. R. Ashill, M. J. Wilson, I. J. Woodcock, C. P. Tilman and K. J. Langan, 2000. Laser doppler anemometry investigation on sub boundary layer vortex generators for flow control. In 10th symposium on application of laser techniques to fluid mechanics, Lisbon**10**.
5. Wheeler, G.O., 1991. Low drag vortex generators. U.S. Patent **5**, 058, 837.
6. Godard, G. and M. Stanislas, 2006. Control of a decelerating boundary layer. Part 1: Optimization of passive vortex generators. Journal of Aerospace Science and Technology, **10(3)**, 181-191.
7. Pauley, W.R. and J. K. Eaton, 1988. Experimental study of the development of longitudinal vortex pairs embedded in a turbulent boundary layer. Journal of American Institute for Aeronautics and Astronautics, **26(7)**, 816-823.
8. Ahmad, K., J. Watterson, J. Cole and I. Briggs, 2005. Sub-boundary layer vortex generator control of a separated diffuser flow. In 35th Journal of American Institute for Aeronautics and Astronautics Fluid Dynamics Conference and Exhibit, 4650.

9. Bur, R., D. Coponet and Y. Carpels, 2009. Separation control by vortex generator devices in a transonic channel flow. Journal of Shock Waves, **19**, 521-530.
10. Lin, J.C., 2002. Review of research on low-profile vortex generators to control boundary-layer separation. Journal of Progress in Aerospace Sciences, **38(4-5)**, 389-420.
11. Lin, J., 1999. Control of turbulent boundary-layer separation using micro-vortex generators. In 30th Fluid Dynamics Conference, 3404.
12. Babinsky, H., N. Makinson and C. Morgan, 2007. Micro-vortex generator flow control for supersonic engine inlets. In 45th Journal of American Institute for Aeronautics and Astronautics Aerospace Sciences Meeting and Exhibit, 521.
13. Jiang, P., Z. Wang and I. Gursul, 2010. Effects of unsteady trailing-edge blowing on delta wing aerodynamics. Journal of Aircraft, **47(2)**, 591-602.
14. Shan, H., L. Jiang and C. Liu, 2005. Direct numerical simulation of flow separation around a NACA 0012 airfoil. Journal of Computers & fluids, **34(9)**, 1096-1114.
15. Velte, C. M., M. O. L. Hansen, and D. Cavar, 2008. Flow analysis of vortex generators on wing sections by stereoscopic particle image velocimetry measurements. Journal of Environmental Research Letters, **3(1)**, 015006.
16. Johansen, S. T., J. Wu and W. Shyy, 2004. Filter-based unsteady RANS computations. International Journal of Heat and fluid flow, **25(1)**, 10-21.
17. Zhen, T.K., M. Zubair and IK. A. Ahmad, 2011. Experimental and numerical investigation of the effects of passive vortex generators on Aludra UAV performance. Chinese Journal of Aeronautics, **24(5)**, 577-583.
18. Sarjito, N. Aklis and T. Hartanto, 2017. An optimization of flap and slat angle airfoil NACA 2410 using CFD. In Journal of American Institute of Physics Conference Proceedings,**1831(1)**, 020038.
19. Julian, J., Harinaldi, Budiarso, C. C. Wang and M. J. Chern, 2018. Effect of plasma actuator in boundary layer on flat plate model with turbulent promoter. Journal of Proceedings of the Institution of Mechanical Engineers, Part G: Journal of Aerospace Engineering, **232(16)**, 3001-3010.
20. Sudhakar, S. and N. Karthikeyan, 2021. Flow Separation Control on a NACA-4415 Airfoil at Low Reynolds Number. In Proceedings of 16th Asian Congress of Fluid Mechanics, 323-334.
21. Yavuz, T., E. Koç, B. Kılkış, Ö. Erol, C. Balas and T. Aydemir, 2015. Performance analysis of the airfoil-slat arrangements for hydro and wind turbine applications. Journal of Renewable Energy, **74**, 414-421.
22. Julian, J., W. Iskandar, F. Wahyuni, A. Armansyah, and F. Ferdyanto, 2022. Effect of Single Slat and Double Slat on Aerodynamic Performance of NACA 4415. International Journal of Marine Engineering Innovation and Research, **7(2)**.
23. Hinze, J.O., 1975. Turbulence, McGrawHill Publishing Co. New York.
24. Chou, P.Y., 1945. On velocity correlations and the solutions of the equations of turbulent fluctuation. Journal of Quarterly of Applied Mathematics, **3(1)**, 38-54.
25. Davidov, B., 1. 1961. On the statistical dynamics of an incompressible turbulent fluid. Journal of Doklady Akademii nauk SSSR, **136**, 47.
26. Harlow, F.H. and P. I. Nakayama, 1968. Transport of turbulence energy decay rate (No. LA-3854). Los Alamos Scientific Laboratory, New Mexico.
27. Jones, W.P. and B. E. Launder, 1972. The prediction of laminarization with a two-equation model of turbulence. International journal of heat and mass transfer, **15(2)**, 301-314.
28. Launder, B.E. and B. I. Sharma, 1974. Application of the energy-dissipation model of turbulence to the calculation of flow near a spinning disc. Journal of Letters in heat and mass transfer, **1(2)**, 131-137.
29. Wilcox, D.C., 1998. Turbulence modeling for CFD. La Canada, CA: DCW industries, **2**, 103-217.
30. Barlow, J.B., W. H. Rae and A. Pope, 1999. Low-speed wind tunnel testing. John Wiley & Sons.
31. Efstratios, S., 1988. The aerodynamic performance of the NACA-4415aerofoil section at low Reynolds numbers. MSc (Research), Department of Aerospace Engineering, University of Glasgow.
32. Fouatih, O. M., M. Medale, O. Imine and B. Imine, 2016. Design optimization of the aerodynamic passive flow control on NACA 4415airfoil using vortex generators. European Journal of Mechanics-B/Fluids, **56**, 82-96.